Asociación Argentina de Astronomía
BAAA, Vol. 55, 2012
A.C. Rovero, G.E. Romero, L. Pellizza & M. Lares, eds.

PRESENTACIÓN MURAL

X-ray structures from outflowing Young Stellar Objects interacting with the Interstellar Medium

Mariana Orellana[1,2], Rosaria Bonito [3], Javier López-Santiago [4],
J. Facundo Albacete Colombo [5], Marco Miceli [3]

(1) Instituto Argentino de Radioastronomía CCT La Plata (CONICET), C.C.5, (1894) Villa Elisa, Buenos Aires, Argentina.
(2) Facultad de Ciencias Astronómicas y Geofísicas, UNLP
(3) Dipartimento di Fisica, Universita' di Palermo, INAF Osservatorio Astronomico di Palermo, P.zza del Parlamento, 1 90134 Palermo, Italy
(4) Departamento de Astrofísica y Ciencias de la Atmósfera, Universidad Complutense de Madrid, E-28040, Madrid, España
(5) Centro Universitario Regional Zona Atlántica (CURZA) Universidad Nacional del COMAHUE, Argentina

Abstract. Young stellar objects (YSOs) are strongly related to winds and outflows. Changes in the morphology and emission properties of those outflows can be the result of their interaction with the Interstellar Medium. The available tools developed into the computational field put at hand a better understanding of the structures that may form on scenarios with growing degrees of complexity. In this work we consider the propagation of a continuously driven supersonic protostellar jet through an inhomogeneous ambient described as an isothermal medium at the base of the launching site and a denser layer far from the YSO. The hydrodynamic evolution, including thermal conduction and radiative cooling is solved, and from the obtained temperature and density distributions we synthetize the outcoming emission in the X-ray band. We then consider the interstellar absorption and the response of the current X-ray telescopes in order to investigate the conditions leading to detectable X-rays.

Resumen. Los objetos estelares jóvenes suelen presentar vientos y flujos colimados. A partir de su interacción con el medio interestelar pueden resultar cambios en su morfología y propiedades de emisión. Las herramientas computacionales actuales ponen a nuestro alcance el estudio de situaciones como esta, con creciente complejidad. En este trabajo consideramos la propagación de un flujo protoestelar contínuo y supersónico a través de un medio con una discontinuidad, siendo más denso en una región lejana a la base desde donde se lanza el flujo. Seguimos su evolución hidrodinámica incluyendo enfriamiento radiativo y conducción térmica, y de las distribuciones obtenidas para la densidad y temperatura, derivamos la emisión saliente en rayos X. Luego consideramos la absorción interestelar y respuesta instrumental de los telescopios de rayos X para indagar las condiciones necesarias para detectar dicha emisión.

1. The model and simulation scheme

We consider the propagation of a continuously driven supersonic protostellar jet with density $n_j = 500$ cm^{-3} and temperature $T_j = 10^4$ K through an isothermal medium at the base of the launching site and a dense layer far from the YSO. This system can be a realistic representation of the observed medium around the protostar L1630MIR-51 that seems to have blown material in direction of the ionization front IC 434. The latter appears as a bright *wall* in the deep Wide Field Camera 3 images, while the origin of the Herbig Haro objects in the vicinity could be ejections from this YSO.

The initial conditions in our model are set to describe pressure equilibrium between the jet and the ambient, and between the ambient and the wall. The basic parameters for this configuration are three:

$$\begin{aligned} M_j &: \text{initial jet Mach number,} \\ \nu_a = n_a/n_j &: \text{initial ambient-to-jet density contrast, and} \\ \nu_w = n_w/n_j &: \text{the initial wall-to-jet density contrast,} \end{aligned}$$

while for for other flow properties defining the scenario we have used characteristic values, similar to Bonito et al. (2004).

The hydrodynamic evolution, including thermal conduction and radiative cooling is solved assuming a perfect, fully ionized, gas with specific heats ratio $\gamma = 5/3$. The usual mass and momentum equations of conservation are considered along with the following energy equation

$$\frac{\partial \rho E}{\partial t} + \nabla \cdot (\rho E + p)\mathbf{v} = -\nabla \cdot q - n_e n_H P(T) \tag{1}$$

with

$$p = (\gamma - 1)\rho\epsilon, \qquad E = \epsilon + \frac{1}{2}|\mathbf{v}|^2, \tag{2}$$

where p is the pressure, E the total gas specific energy (internal energy, ϵ, and kinetic energy) respectively, ρ is the mass density, t the time, $\mathbf{v}$ the plasma velocity, q the heat flux, and $P(T)$ is the radiative losses function per unit emission measure which takes into account free-free, bound-free, bound-bound and 2 photons emission (Raymond & Smith 1977, Mewe et al. 1985, Kaastra & Mewe 2000). The other quantities have the typical meaning. An interpolation expression for the thermal conductive flux allows for a smooth transition between the Spitzer and saturated conduction regimes (Dalton & Balbus 1993).

Any magnetic field is regarded as negligible. We have fixed the initial jet radius $r_j = 100$ AU. The wall is located at $z = 10^4$ AU, and the computational domain is axisymmetric with $(r \times z) \simeq (1500 \times 15000)$ AU. Reflection boundary conditions are imposed along the jet axis, inflow boundary conditions at the base for $r < r_j$, and outflow boundary conditions elsewhere. The calculations are performed with the FLASH code (Fryxell et al. 2000), which incorporates an adaptive grid scheme to handle compressible plasmas with shocks, and uses the message passing interface library to achieve parallelization.

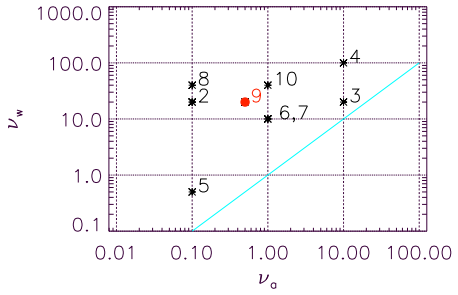

Figure 1. One plane of the explored parameter space. From the resulting temperature the configurations 7 and 10 produce too hot front shocks.

2. Results and emission properties

In order to explore the parameter space we have followed the evolution of the jet for several configurations designed to represent realistic HH flows and keeping $n_w > n_a$ through different combinations. A variety of temperature distributions[1] are achieved after a time interval between ~ 100 and ~ 300 yr, depending on the set of parameters, when the shock front has advanced inside the wall upto a half of its height. We then consider the interstellar absorption for a column density $N_H \sim 10^{22}$ cm^{-2}, and the response of the last generation X-ray telescopes to obtain the focal plane image. Specifically, we use Chandra to compare images and XMM-Newton to compare the results from the spectral analysis, in order to take advantage of the high spatial resolution of the former and the large effective area of the latter.

The best suited case to produce an X-ray source detectable at the assumed distance, $d \sim 400$ pc, is given by $M_j = 40$, $\nu_a = 0.5$, and $\nu_w = 20$. These values correspond to run 9 indicated in red in Figure 1 where we show one of the parameter planes explored. In Figure 2 we show the synthetic image, and the spectrum. The obtained luminosity is $L_X \sim 10^{30}$ erg/s. For the run 9 configuration and ~ 100 yr of advance the X-ray source is located inside the wall and has an almost pointlike morphology.

Acknowledgments: This research has been supported by the Argentine agency ANPCyT through Grant PICT 2010-0213.

References

Dalton, W.W. & Balbus, S.A. 1993, ApJ, 404, 625
Bonito, R., Orlando, S., Peres, G., Favata, F., Rosner, R. 2004, A&A, 424, L1
Fryxell, B., Olson, K., Ricker, P., et al. 2000, ApJS, 131, 273, `http://flash.uchicago.edu`
Kaastra, J.S. & Mewe, R. 2000, *Atomic Data Needs for X-ray Astronomy*

[1]The distributions are not shown here but the authors will be pleased to shown them as they were included in the poster for the meeting. Contact: *morellana@fcaglp.unlp.edu.ar*

Mewe R., et al. 1985, A&AS, 62, 197
Raymond, J.C. & Smith, B.W., 1977, ApJS, 35, 419

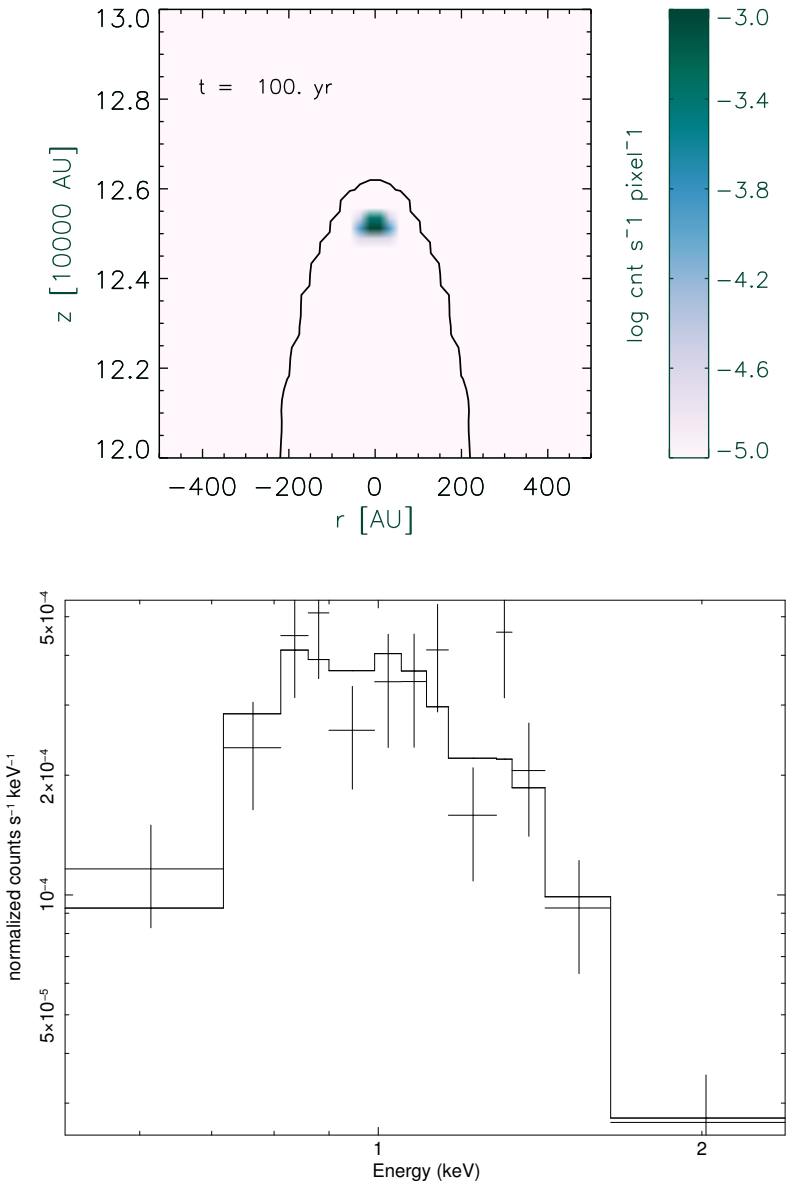

Figure 2. Top: Synthetic X-ray map. Detail showing the source is located behind the shock. The black contour indicates the place of not perturbed gas of the wall. Bottom: The X-ray spectrum using an exposure time 500 ks, binning to have at least 10 counts per bin. The model shows the C-statistic fit, which resulted in $kT = 0.28$ keV.

Asociación Argentina de Astronomía
BAAA, Vol. 55, 2012
A.C. Rovero, G.E. Romero, L. Pellizza & M. Lares, eds.

PRESENTACIÓN MURAL

Compact Stars in R-Squared Gravity

Federico García[1,2], Florencia A. Teppa Pannia[2], Mariana Orellana[1,2], Gustavo E. Romero[1,2]

(1) Instituto Argentino de Radioastronomía CCT La Plata - CONICET, C.C.5, (1894) Villa Elisa, Buenos Aires, Argentina.
(2) Facultad de Ciencias Astronómicas y Geofísicas, UNLP, Paseo del Bosque s/n, B1900FWA La Plata, Argentina.

Abstract. Recent progress in testing certain modified-gravity theories has been achieved by the study of the structure of compact objects like Black Holes and Neutron Stars (NSs). In particular, it is possible that the *squared*-gravity generalization of the Lagrangian density, given by the function $f(R) = R + \alpha R^2$, may yield acceptable models for heavier NSs than General Relativity (GR) does.

In the strong gravitational regime, the differences among alternative gravity theories should be enhanced. Because of the complexity of the field equations, perturbative methods are required to approach solutions. In this work, we calculate the structure of both NSs and Quark Stars (QSs) focusing on the behaviour of their interior profiles, compared to those from GR. We find that these profiles depend on high-order derivatives of the Equations of State (EoSs), showing regions where the enclosed mass decreases with the radius in a counter-intuitive way.

Resumen. En los últimos años se han registrado avances en la verificación de teorías de gravedad modificada a través del estudio de la estructura de objetos compactos. En particular, es posible que la generalización *cuadrática* de la densidad lagrangiana, dada por la función $f(R) = R + \alpha R^2$, permita modelar estrellas de neutrones más masivas que las admitidas por la Relatividad General (RG).

En el régimen de campo gravitacional fuerte, las diferencias entre teorías alternativas de la gravedad deberían amplificarse. Debido a la complejidad de las ecuaciones de campo, se requieren métodos perturbativos para aproximar las soluciones. En este trabajo calculamos la estructura de estrellas de neutrones y estrellas de *quarks* enfocándonos en el comportamiento de los perfiles interiores resultantes, y comparándolos con sus equivalentes en RG. Encontramos que estos perfiles dependen de las derivadas de order superior de la ecuación de estado utilizada, mostrando regiones donde la masa encerrada decrece con el radio, de modo contraintuitivo.

1. Introduction

The appearance of Extended Theories of Gravity was strongly stimulated by the possibilities they migth provide to reinterpret the current cosmological data (de Felice & Tsujikawa 2010; Sotiriou & Faraoni 2010) without involving non-standard matter in the energy-momentum tensor. We focus our work on the so-called $f(R)$-gravity theories, which are based on a modification of the Einstein-Hilbert action: the usual Lagrangian density is generalized replacing the Ricci curvature scalar, R, by a function of it or by a combination of high-order invariants of the curvature tensor (see, for instance, Capozziello & Faraoni 2011).

The simplest choice $f(R) = R + \alpha R^2$, also called "R-squared" gravity, had been further studied as a viable alternative cosmological model. But in contrast to gravity in the weak-field regime, gravity in the strong-field regime is largely unconstrained by observations (e.g. DeDeo & Psaltis 2003). Under this motivation, we investigate in detail the structure of NSs and QSs in R-squared gravity, using a perturbative approach (Babichev & Langlois 2010).

2. Structure equations in *R-squared* gravity

Modified TOV equations can be obtained from the gravitational field equations, assuming spherical symmetry and staticity. In the metric formalism, the variation of the action with respect to the metric yields fourth-order differential equations. We adopt the perturbative approach presented in Cooney et al. (2010) to solve them in the case that $f(R) = R + \alpha R^2 = (1 + \beta)R$, where the dimensionless quantity $\beta \equiv \alpha R$ comprises the deviation from GR and the perturbative method is applied as long as $|\beta| \ll 1$.

In this approach, functions in the metric are expanded into a leading term, denoted with subscript 0, plus a corrective one (subscript 1) that is of first order in β. Following Arapoğlu et al. (2011), the hydrodynamic quantities are also defined perturbatively: $\rho = \rho_0 + \beta\rho_1$ and $p = p_0 + \beta p_1$, and the mass is defined assuming that the solution for the metric has the same form as the exterior Schwarzschlid solution in GR. With this considerations, and taking into account that ρ_0 and p_0 satisfy Einstein's equations, the derived modified TOV equations are:

$$\frac{\mathrm{d}m}{\mathrm{d}r} = 4\pi r^2\rho - 2\beta\left[4\pi r^2\rho_0 - \frac{c^2}{8G}r^2R_0 + \left(2\pi\rho_0 r^3 - \frac{c^2}{G}r + \frac{3}{2}m_0\right)\frac{R_0'}{R_0} - r\left(\frac{c^2}{2G}r - m_0\right)\frac{R_0''}{R_0}\right]$$

$$\frac{\mathrm{d}p}{\mathrm{d}r} = \frac{c^2\rho + p}{2Gm - c^2 r}\,G\left\{\left(\frac{4\pi}{c^2}r^2p + \frac{m}{r}\right) - 2\beta\left[\frac{4\pi}{c^2}r^2p_0 + \frac{c^2}{8G}r^2R_0 \;+\left(\frac{2\pi}{c^2}p_0r^3 + \frac{c^2}{G}r - \frac{3}{2}m_0\right)\frac{R_0'}{R_0}\right]\right\}$$

where we use the prime for radial derivatives. Here the terms 2β [...] indicate the first order correction. Note that in order to work up to first order in β, the brackets have been evaluated at order zero. The α parameter is constrained to the values reported by Santos (2010), and references therein, which points to 10^8 cm$^2 < \alpha/3 < 10^{10}$ cm^2.

2.1. Equations of State and the numerical method

We calculate the mass-radius ($M_\star - R_\star$) relations for NSs, considering two different EoSs: SLY (Haensel & Potekhin 2004) and POLY (Silbar & Reddy

2004). The first one is a realistic EoS that represents the behaviour of nuclear matter at high density, but has a complex analytical representation and the error propagation of its derivatives is out of our knowledge. The second EoS is a simple polytropic approximation, $p \propto \rho^2$, and allows us to study zeroth-order modified gravity effects, separating them from more tricky issues arising from the analytical representation of the realistic EoS. The interior of QSs is represented by a SQM EoS, $p = (c^2\rho - 4B)/3$, assuming a typical value of $B = 60$ MeV fm^{-3} for the MIT bag constant (Glendenning 2000; Degrand et al. 1975).

3. Results and Conclusions

In Fig. 1 we show the mass-radius ($M_\star - R_\star$) relations using SLY, POLY and SQM EoSs, obtained for seven values of the α parameter between –0.2 and +0.2 km^2, and considering central densities, ρ_c, running from $10^{14.6}$ gr cm^{-3} to $10^{15.9}$ gr cm^{-3}. SLY EoS configurations are more sensitive to the value of α parameter than the others.

In the right-bottom panel of Fig. 1 we show the radial profiles obtained for the density, $\rho(r)$, and mass, $m(r)$, for $\alpha = -0.2$, 0.0 and +0.2 km^2 with the SLY EoS. Although the density, and hence the pressure, follow rather usual (resembling GR) profiles, the effects of $f(R)$ are reflected in the mass profiles and are evident close to the NS surface (i.e. at $r \sim 10$ km, for $\rho_c = 10^{15.4}$ gr cm^{-3}) where, in a narrow layer ($\Delta r \sim 0.2$ km), an unexpected (counter-intuitive) decrease in $m(r)$ appears before ($\alpha > 0$) or after ($\alpha < 0$) a dip (peak) in the profile. In the frame of GR, this effect could only be explained by means of a negative-density fluid, while in $f(R)$ theories, it arises as a natural consequence of the coupled space-time geometry and matter content. On the contrary, adopting a simple polytropic EoS for NSs and QSs, no anomalous behaviour of the internal profiles of the stars is observed. Hence, because these particular effects arrive as a direct consequence of the high-order derivatives of realistic EoSs, it is important to remark that the uncertainties on the analytical representation of the EoS adopted could have an enhanced effect on the $f(R)$ solutions.

Our most important result concerns the detailed study of the internal structure of NSs considering the largest acceptable values for the α parameter (i.e. the stronger perturbation allowed to GR by the actual constraints in R-squared gravity). We find that a combination between the metric behaviour and the high-order derivatives of the realistic EoS leads to a region where the mass enclosed in a spherical region of the star decreases with the radius in a counter-intuitive way.

Acknowledgments. The authors appreciate helpful comments from Prof. Santiago E. Pérez Bergliaffa. M.O. acknowledge support by the Argentine Agency CONICET and ANPCyT.

References

Arapoğlu S., Deliduman C., Yavuz Ekşi K., 2011, JCAP, 7, 20
Babichev E., Langlois D., 2010, Physical Review D, 81, 124051
Capozziello S., Faraoni V., 2011, Beyond Einstein Gravity. A survey of Gravitational Theories for Cosmology and Astrophysics. Springer Science+Business Media

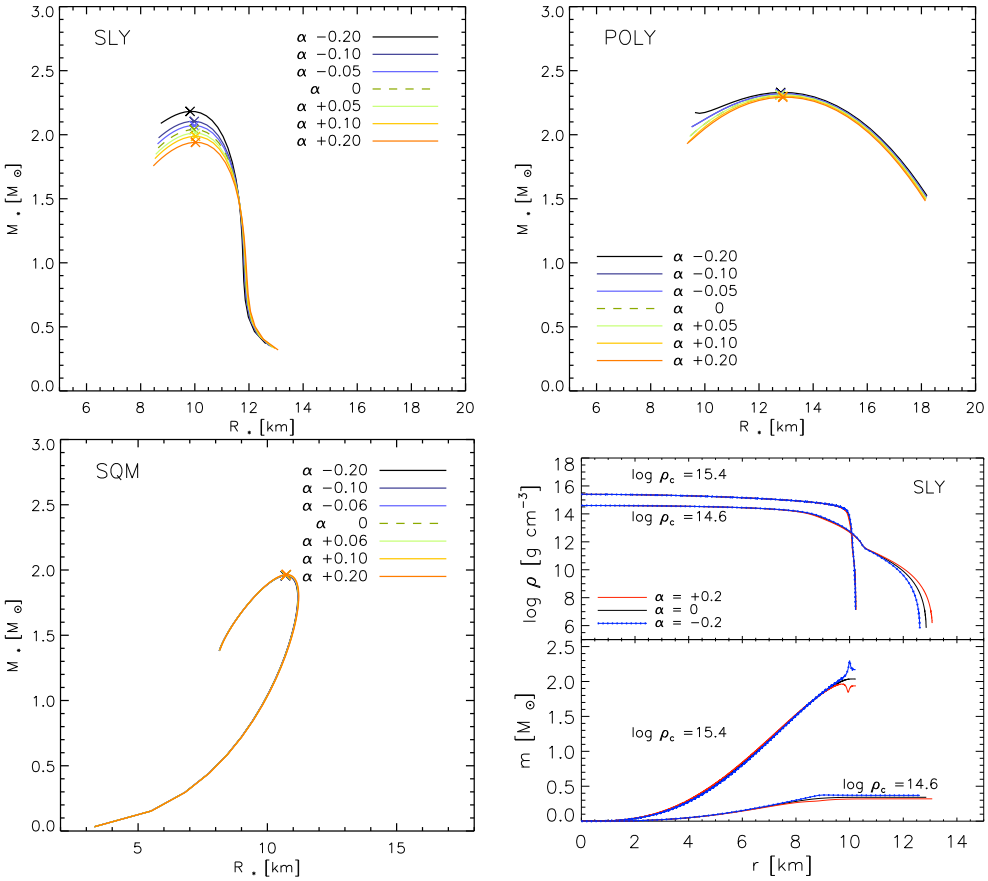

Figure 1. Mass-radius ($M_\star - R_\star$) relations for the three selected EoS. Crosses indicate the maximum mass for each curve, assuming a necessary condition for equilibrium: $\mathrm{d}M/\mathrm{d}\rho_c > 0$. Internal structure profiles of NSs with SLY EoS are shown in the bottom-right panel.

Cooney A., Dedeo S., Psaltis D., 2010, Physical Review D, 82, 064033
de Felice A., Tsujikawa S., 2010, Living Reviews in Relativity, 13, 3
DeDeo S., Psaltis D., 2003, Physical Review Letters, 90, 141101
Degrand T., et al., 1975, Phys.Rev.D, 12, 2060
Glendenning N. K., ed. 2000, Compact stars: nuclear physics, particle physics, and general relativity
Haensel P., Potekhin A. Y., 2004, A&A, 428, 191
Santos E., 2010, Physical Review D, 81, 064030
Silbar R. R., Reddy S., 2004, American Journal of Physics, 72, 892
Sotiriou T. P., Faraoni V., 2010, Reviews of Modern Physics, 82, 451

Asociación Argentina de Astronomía
BAAA, Vol. 55, 2012
A.C. Rovero, G.E. Romero, L. Pellizza & M. Lares, eds.

PRESENTACIÓN MURAL

The Cherenkov Telescope Array: status and perspectives

M. C. Medina[1], M. Orellana[1] & G. E. Romero[1]

(1) Instituto Argentino de Radioastonomía (CONICET)

Abstract. The progress of the ground-based γ-ray Astronomy in the last 10 years (mainly due to instruments such as H.E.S.S., MAGIC and VERITAS) has inspired the scientific community to go for the next step in the evolution of the ground-based Imaging Atmospheric Cherenkov Technique (IACT). CTA has been conceived as an array of Cherenkov telescopes working as an open observatory, covering a wide energy range ($\sim$ 30 GeV to 100 TeV), with an enhanced sensitivity and improved spatial, temporal and energy resolution. The design phase of CTA has been completed and the project is in the middle of its preparatory phase. The begin of the construction is foreseen for 2014. In this paper we describe the status of the project, the technical challenges and we give an insight on the involved physics.

Resumen. El avance de la Astronomía de rayos γ desde Tierra en los últimos 10 años (principalmente gracias a instrumentos como H.E.S.S., MAGIC y VERITAS) ha inspirado a la comunidad científica para dar el próximo paso en la evolución de la Técnica de detección del Cherenkov atmosférico(IACT). CTA ha sido concebido como un arreglo de telescopios Cherenkov para cubrir un amplio rango de energías con una sensibilidad y resolución angular y energética muy superior a la de los instrumentos actuales. La etapa de diseño de CTA ha sido completada y el proyecto se encuentra en la etapa de "preparación" antes del comienzo de la construcción, planificada para 2014. En este trabajo se describe el status del proyecto y de los desafíos tecnológicos que se presentan además de una breve introducción a la física involucrada.

1. Introduction

Very-high energy (VHE) γ-rays are produced in non thermal processes in the universe, namely in galactic objects like pulsars, pulsar-wind nebulae (PWNe), supernova remnants (SNR), microquasars, etc . Among the extragalactic VHE γ-rays sources are active galactic nuclei (AGN), Gamma-Rays Bursts (GRB) and starburst galaxies.

Ground-based γ-ray astronomy has already demonstrated to be a mature scientific technique to probe non-thermal phenomena in the universe. Upon reaching the Earth's atmosphere, VHE γ-rays interact with atmospheric nuclei and generate electromagnetic showers. The charged secondary particles, mostly electrons and positrons, move with ultra-relativistic speed and emit Cherenkov

light. This radiation is mainly concentrated in the near UV and optical band and is collected by telescopes mirrors and focused onto multi-pixel cameras that record the shower images.

This field has been impulsed by the Whipple Collaboration, which discovered the first source of TeV γ-rays (the Crab Nebula) in 1989. Since then, results from the latest generations of telescopes have revealed a rich sky with different objects emitting VHE γ-rays (Buckley et al. 2008). More than 100 sources at TeV are known so far, detected with the ground-based instruments as H.E.S.S.[1], MAGIC[2] and VERITAS[3].

In the GeV domain, the Fermi/*LAT*, has discovered more than 1800 bright sources (20 MeV to 100 GeV) during the first 3 years of operation (Nolan et al. 2012).

2. CTA: a new science infrastructure

CTA is formed by two large arrays of Cherenkov telescopes of different sizes, based on proven technology and deployed on an unprecedented scale. See the left panel of Fig.1 for an artistic view of the array configuration. It was conceived as a new facility, with capabilities well beyond the existing instruments and their possible upgrades.

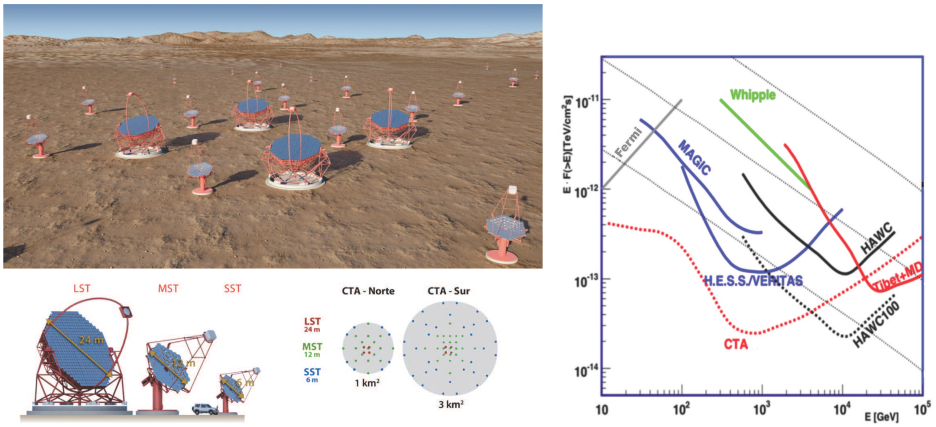

Figure 1. *Left:* Possible layout of the composite CTA Observatory. *Right:* Integral sensitivity for a Crab-like spectrum for several current IACT and expected for CTA (5σ, 50 h) and Fermi/LAT (5σ, 1 yr).

This project unites the main research groups in this field in a common strategy. The Consortium is composed nowadays of 25 countries and more than 100 institutions are implicated. CTA will, for the first time in this field, provide open access via targeted observation proposals and generate large amounts of

[1]http://www.mpi-hd.mpg.de/hfm/HESS/
[2]http://magic.mppmu.mpg.de/
[3]http://veritas.sao.arizona.edu/

public data, accessible using Virtual Observatory tools. CTA aims to become a milestone in a networked multi-wavelength exploration of the high-energy non-thermal universe.

2.1. Science motivation

CTA science prospectives are wide (for more detailed discussion see Actis et al. 2011 and Aharonian et al. 2008), but they are based on three cornerstones:
The origin of cosmic rays (CR) and their role in the Universe. Is commonly said that CR are accelerated in shocks generated by supernova explosions. γ-ray emission is detected in several SNR but the nature of the underlaying processes is not yet wholly understood. A deep CTA survey of the Galactic plane should unveil a handful of PeVatrons (not yet discovered) and of other types of CR accelerators candidates as PWNe, pulsars and binaries. The impact of the accelerated particles on their environment will be studied as CTA will enable detailed mappings of VHE emission around potential CR accelerators (Acero et al. 2013).
The nature of particle acceleration around black holes (BH), in particular inside objects as AGN. CTA will be able to detect a large number of these objects enabling population studies. It will be also possible to probe variability time scales well below minutes, putting constraints on acceleration and cooling times in these types of sources. A detailed study of the Extragalactic background light, and the emission from galaxy clusters and Gamma Ray Burst will be also possible by means of CTA (Sol et al. 2013).
Physics beyond the horizon. It is difficult to speculate about the unknown, and definitely we cannot accurately predict how much CTA will unveil about any physics that is beyond our standard model of the world. γ-rays, however, hold the potential to reveal properties of the elementary particles that make up our Universe because photonic signatures of particle interactions, decays and annihilations show up in this energy range (Martinez 2009, Bertone 2010).

2.2. An instrument of "unprecedented" performance

This observatory aims to provide full-sky view, from a southern and a northern site and to have the following characteristics:
-A sensitivity 10 times greater than any existing instrument. It will allow detection and in-depth study of large samples of known sources and it will be also sensitive to new phenomena. See the right panel of Fig.1.
-Coverage of three to four orders of magnitude in energy range, for distinguish between an hadronic or leptonic origin of VHE emission in different scenarios.
-Angular resolution in the arc-minute range, which is 5 $\times$ better than the typical values for current instruments.
-Time resolution of less than minute, for resolving flaring and variable emission.
-Wide range of configurations for observation, for the study of individual objects with high sensitivity, and the simultaneous monitoring of tens of flaring objects.
-Survey capability dramatically enhanced. For the first time, a full-sky survey at high sensitivity will be possible.

2.3. Technical Challenges

Three sizes of telescopes will be placed in different configurations and covering areas related to the desired sensitivity (see the left panel of Fig. 1: SST –

Small size telescopes of 5-8m diameter–; MST –Medium size telescopes of 10-12m diameter–; and LST –Large size telescopes of 20-30m diameter–.

Few LSTs should observe the sub-100 GeV photons thanks to their large reflective area. They will have a parabolic shape to avoid the intrinsic optical aberrations and will have limited Field of View (4° or 5°). This means the technical challenge of displacing the camera at more than 28 m from the reflector. Several tens of MSTs will perform the bulk TeV search. Different designs are currently under study and the construction of the first prototype is ongoing. Finally, various tens of SSTs will complete the array to perform the super-TeV search. They shall be simple in construction and should have moderate cost. A dual mirror telescope design is under study (Guarino et al. 2009). These telescopes are going to be distributed covering a multi-km^2 area.

A major effort is currently focused on the telescope design, the mirror facets development and the electronic and focal plane instrumentation. Different projects for SSTs, MSTs and LSTs are under design at several institutes to stimulate competition and technological development. Mirrors constitute an important challenge because they contribute to a considerable part of the costs. The focal plane instrumentation also represents a challenge in technology and cost. The efficiency of the collection of Cherenkov photons and their conversion to photoelectrons in the photosensor must be improved. Finally, enlarging the energy range requires appropriate electronics with a sufficiently large dynamic range.

3. Summary

The CTA observatory is the logical next step in the exploration of the high-energy Universe and will promote VHE observations to a public tool for modern astronomy. CTA will explore the VHE domain from several tens of GeV up to more than 10 TeV with unprecedented sensitivity and angular resolution, enabling a comprehensive understanding of cosmic particle acceleration physics at various scales, distances and time scales. CTA is passing through the preparatory phase for the construction and operation, dedicated to the development and prototyping. In about 5 years from now, CTA will produce its first results starting the next era on the VHE γ-rays astronomy.

Acknowledgments. We gratefully acknowledge support from the agencies and organizations listed in this page: http://www.cta-observatory.org/?q=node/22

References

Acero F., et al., 2013, Astroparticle Physics, 43, 276
Actis M., et al., 2011, Experimental Astronomy, 32, 193
Aharonian F., et al., 2008, Reports on Progress in Physics, 71, 096901
Bertone G., 2010, Particle Dark Matter : Observations, Models and Searches. Cambridge University Press
Buckley J., et al., 2008, ArXiv e-prints
Guarino V. et al. 2009, in APS Meeting, "The Advanced Gamma-ray Imaging System"
Martinez M., 2009, Journal of Physics Conference Series, 171, 012013
Nolan P. L., et al., 2012, ApJS, 199, 31
Sol H., et al., 2013, Astroparticle Physics, 43, 215